

# Layout, Validation and Benchmark of an all new Frontal Offset Barrier FEM Model

Bernhard Fellner<sup>1</sup>, Thomas Jost<sup>2</sup>

<sup>1</sup>Magna Steyr Fahrzeugtechnik AG & CoKG, Graz, Austria

<sup>2</sup>Kompetenzzentrum – Das Virtuelle Fahrzeug Forschungsgesellschaft mbH, Graz, Austria

## Summary:

For the customer, passive safety is one of the driving reasons for the decision when buying a new car. To ensure high safety standards, passive safety is demonstrated in vehicle crash tests. Instead of vehicle to vehicle crash tests, one vehicle is replaced by an aluminium honeycomb based crash barrier. This barrier represents the front of a vehicle by the shape, the deformation behaviour and the energy absorption. Using Finite Element Method (FEM) it is possible to show and predict the behaviour of the vehicle's structure during a previous mentioned crash test. To ensure good simulation results compared to reality it is not only necessary to correctly build up the FE model of the vehicle, but to simulate the real behaviour of the crash barrier too. Experience shows that the deformation behaviour of the FEM crash barrier seriously influences the quality of the full vehicle simulation. The barrier models that are currently in use, show insufficient reliable results. The modelling techniques are not able to show the principle deformation and failure behaviour of aluminium honeycomb. Moreover huge barrier deformation is able to cause serious instability problems of the models. That leads to an inaccuracy in predicting the vehicle safety during a virtually based development process. It has to be considered that CAE driven design processes are only feasible when the simulation delivers results with reliable prognosis quality.

During the last years a new modelling method for aluminium honeycomb structures especially based on the IIHS side impact barrier was developed. In the meanwhile the method proved to work also with the high relative deformations that have to be faced in a frontal offset crash test. A very specific sequence of tests was carried out to determine the structural properties of the aluminium honeycomb, the cladding and the whole barrier itself as well. The tests were planned to show the reproducibility of the results but also for example the dependence on the test velocity at the same energy levels.

The output of this process is a stable barrier model capable to show localized deformations. This prevents overestimation of energy absorption by distributing the deformation on the whole barrier. The developed method to simulate crash barriers contributes to the improvement of full vehicle crash simulations. Reliable calculation results based on more accurate barrier models will help to reduce the risk of changes in already released toolings after analysing first real crash results.

## Keywords:

Aluminium honeycomb, discrete beam elements, automotive crashworthiness, frontal impact, ODB, crash, barrier;

## 1 Introduction

Vehicle safety is one of the key issues for consumers in their decision for a new car. But also parliaments and consumer organisations focus on the goal to make our roads safer. 2008 was the year with the least fatalities in Germany since 1950 [1]. The amount of crash tests described in laws or by consumer organisations is ever increasing. In addition to that efficient development strategies require reducing the number of prototype generations. For some parts in the future development process of a car there will be no prototype tooling any more. Tests can be performed only after a final release. Only small changes will be possible and therefore costs for changes will be tremendous. Apart from the crash performance the whole vehicle has to be also weight and cost optimised at the same time. These tough goals require very precise development tools already in early phases of the process. Finite Element Method (FEM) proved to be a helpful tool in many disciplines like acoustic, stiffness and crash.

Many of the above mentioned crash tests utilise aluminium honeycomb shaped crash barriers to represent the crash opponent. These barriers have defined shapes and load levels in order to resemble stiffness and shape of vehicles. The stiffest barrier currently in use represents in size and weight a typical American SUV hitting the side of the tested car [2]. Being the boundary condition of the crash the barrier has to be well described in FEM. Any mismatch in stiffness or deformation mode leads to a number of mismatches in the following calculation result. The barrier is only one element in a chain leading to the evaluated biomechanical ratings of the dummy. But it is for sure one of the most important. Therefore FEM barrier models have to be carefully validated and reliable to ensure the required prognosis quality [3].

## 2 Barrier Models in FEM

Aluminium honeycomb structures used in crash barriers are anisotropic hexagonal structures made of thin aluminium foils. Caused by the structural shape, three principle directions T/L/W are observed. The T-direction has the highest load capability while L and W-directions are approximately 10 times weaker [4] [5] [6]. Along these principle directions different characteristic deformation modes can be shown. Additional to global deformation modes aluminium honeycomb structures allow localized deformation. Locally impacted by an intruding body, only the loaded structure deforms. The surrounding not loaded structure remains undeformed [7]. This effect can be observed in frontal crash barriers that usually are loaded only partly by the hitting vehicle as can be seen in figure 1.

Apart from the honeycomb structure failure and rupture of the cladding sheets and disconnection of the glued parts proved to be essential on the overall barrier performance. An ideal barrier model is capable of describing all these effects



Figure 1: Offset Frontal Crash Barrier after Test

### 2.1 State of the Art

State of the art aluminium honeycomb models are based on 8-nodes solid elements [8]. With solids, a honeycomb structure is modelled as a continuum. This loss of structural information leads to inaccuracy of the FE-model. The solid based model is not able to show principle, in-plane (L, W) deformation modes of real honeycomb structures. With special settings the characteristic buckling

mode can be realized in global T-direction [9]. Nevertheless, it is not yet possible to reproduce the typical deformation behaviour of locally loaded honeycomb structures.

Despite the mentioned problem to show principle deformation modes with solid elements, it is possible to validate force-deflection or acceleration curves in a qualitative manner. Solid element based crash barrier models can at first sight show good results when crashed with full vehicle models. Although the simulated results seem to be quite good, the inaccurate deformation behaviour falsifies the in detail force transmission to the tested specimen. It is hardly possible to develop the vehicle's restraint systems based on the simulated results of the wrong loaded car structure. In fact, there is no possibility to ensure the prognosis quality of the virtually driven vehicle safety design process based on such a barrier.

As a consequence in [10] and [11] honeycomb models made of shell elements were presented in crash barrier models. The shell elements are used to directly model the honeycomb structure itself. By this method good results are achieved. Hence there is no loss of structural information in principle. The main problem of shell based honeycomb models is the small required discretisation of each edge of the hexagon. To reach the right force level deformation has to show characteristic buckling modes in T-direction. In FEM the folding process of each cell wall during buckling strongly depends on the amount of elements per cell wall used. More elements lead to better results, because the buckling mode will be shown more realistic. Nevertheless due to the enormous number of elements CPU-time increases a lot compared to solid element barriers.

## 2.2 Discrete Beam Method (DBM)

The DBM was already presented in combination with the IHS Barrier Model [12]. In comparison to a shell based honeycomb model, the DBM leads to a simplified structured model of the hexagonal structure. In contrast to the shell method, each edge of the hexagon is resolved only with one element. Moreover, an increased cell size in order to reduce the amount of elements can be realised quite simple (macro cells). All discrete beams of the model are assigned to characteristic element groups that depend on the principal beam orientation T, L, W of the honeycomb structure.

In general, the DBM allows simulating qualitatively the real characteristic deformation behaviour of honeycomb structures. First, this advantage is based on the ability to set up the load-deflection behaviour of all 6 DOFs. Secondly, each characteristic deformation mode observed is related to an element group. In Figure 2 the deformation behaviour of a DBM model under compressive and mixed (compression and shear) load is shown. In global T-direction, the beam elements fold in a locally layered manner. In principle, this deformation mode approximates the real behaviour of the structure. A mixed compression and shear load results in damaged areas on the top and bottom surface, while the rest remains nearly stable, which is the real characteristic deformation behaviour. Additionally to realistic global behaviour of the DBM model, local deformation behaviour can be modelled (Figure 3). As in reality, only the locally loaded structure will be damaged. In fact, the ability of realistic local failure of the model is the main advantage of the DBM. Exactly these abilities are required to represent honeycomb deformations of offset deformable barriers (ODB).

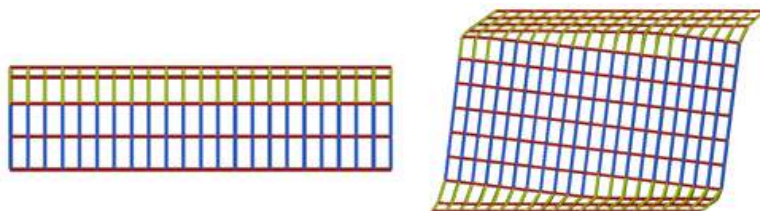


Figure 2: Characteristic deformation behaviour of T- and mixed directional loaded honeycomb model

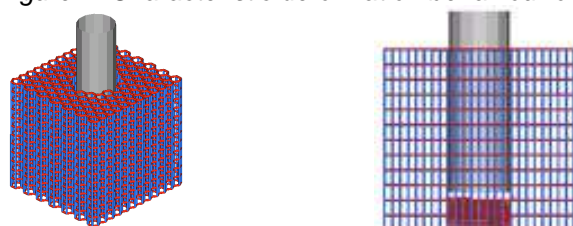


Figure 3: Characteristic deformation behaviour of T-directional locally loaded honeycomb model

## 3 Testing

### 3.1 Test Setup

To fully describe the barrier model a number of tests had to be performed starting with static tests to describe the main honeycomb's material properties. The bumper characteristics have already been tested while building up the IIHS Side impact model. Material models for the cladding were defined including a failure formulation. Details on the process and the material card properties were already presented last year [13]. Following the process described by Jost [12] also system and whole barrier tests had to be performed in order to describe the combination of all the components.

The layout of these tests was limited by the boundary conditions of the test facility. Due to the maximum height of the slope a maximum velocity of approximately 22 kph could be reached. The mass of the trolley was limited to around 2.5 tons. Two strategies were followed in the layout of the dynamic tests. On the one hand a maximum of deformation according to the setup was aimed. On the other hand mass and velocity were varied at the same energy level to investigate the influence of dynamic effects on aluminium honeycomb structures [7].

#### 3.1.1 Static tests

Samples of 200x200x200 mm<sup>3</sup> were statically tested in T-, TL- and TW-direction and used to setup the principal DBM parameter [12].

#### 3.1.2 Full Overlap

The first dynamic test setup was chosen to see mainly uniform axial deformation without failure of either cladding or gluing. As can be seen in figure 4 the barrier was cut in half. This had two major advantages. On the one hand the absorbed energy was less. On the other hand the number of test samples could be increased without raising barrier costs.

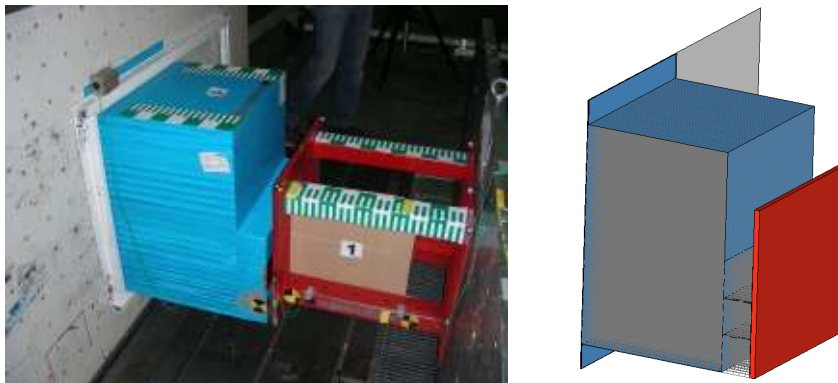


Figure 4: Full overlap setup

#### 3.1.3 Partial Overlap

The second dynamic test (figure 5) should represent conditions similar to a full vehicle crash, where only parts of the barrier are hit. Disconnection of the bumper and of the cladding from the main block could be observed.

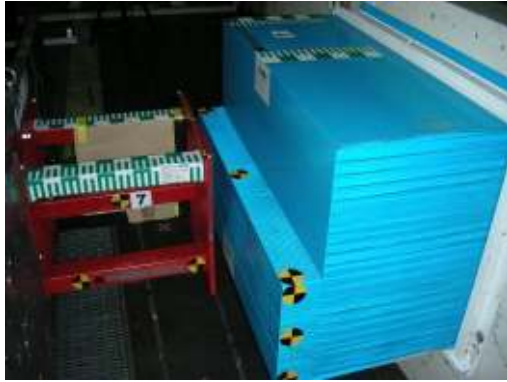
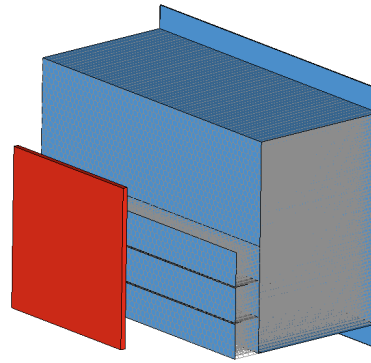


Figure 5: Partial Overlap setup

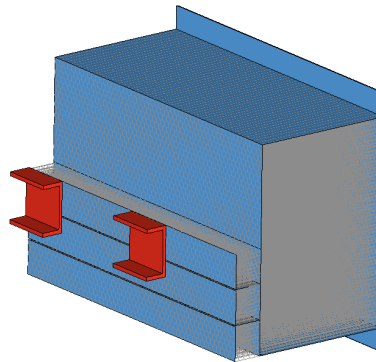


### 3.1.4 Local I-Beam intrusion

The third test setup was meant to only locally destroy the barrier aiming to represent the following situation. With some vehicles it can happen that the barrier gets split by a first local contact and thus is not able to absorb an adequate amount of energy. As can be seen in figure 6 the two impacting areas were positioned to hit one and a half bumper elements in height. The left area was positioned at the border of the barrier, whereas the right one was positioned close to the centre of the barrier.



Figure 6: Local I-Beam setup



## 3.2 Test Data Interpretation

Apart from high speed movies the main data acquisition was carried out via several accelerometers positioned on the trolley. There were positions close to the impacting area but also in the COG and the outmost positions of the trolley. Nevertheless all signals showed significant noise (figure 7). The signals needed to be physically interpreted. The height and slope of the first peak can be massively influenced by the data treatment. Therefore many ways of signal preparation were investigated: for example FFT to filter Eigen-frequencies of the trolley system. After optimising the signal treatment with respect to all three load cases the signal was close to what a plain CFC60 would deliver.

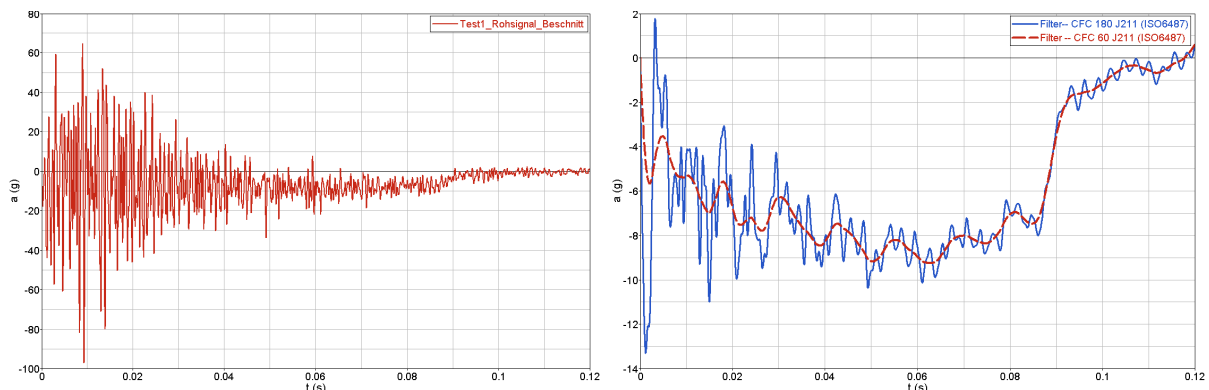


Figure 7: Test Signal from trolley (full overlap), filtered Signal (CFC 180 and CFC 60)

## 4 Validation of EEVC Barrier Model

### 4.1 Full overlap

Three variants with different mass and impact velocity were performed. The first two of which have the same kinetic energy to be absorbed in the barrier (see table 1):

Table 1: Full Overlap Test Conditions

Test No.	Mass [kg]	Velocity [kph]	Energy [kJ]	Colour
Test 1, 2:	1505.5	21.7	27.4	(blue)
Test 3, 4:	2518.5	17.1	28.3	(green)
Test 11, 12:	2518.5	22.1	47,5	(red)

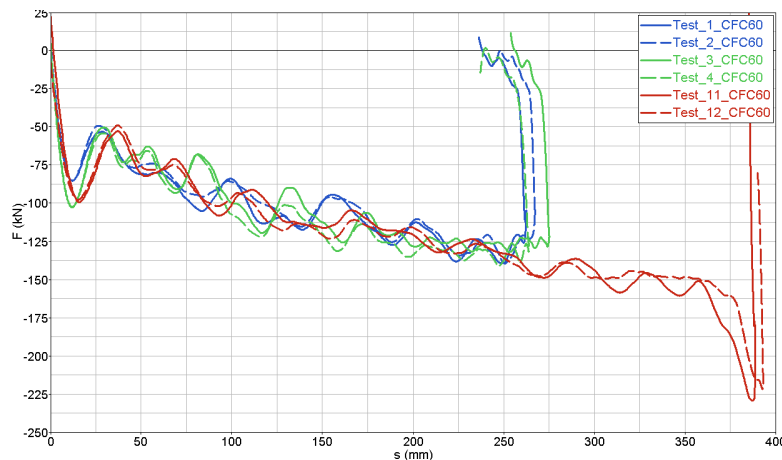


Figure 8: Force /Displacement comparison of the three above mentioned variants

As already shown previously there is only little difference in the force level between the different velocities (figure 8) with strain rates ranging from 10 to 13.7 s<sup>-1</sup> [7].

Below there is the comparison of the FEM results with Test 1 and 2. The green line in the following figures represents the DBM model, whereas blue and black are the test results. As can be seen in figure 9 variance of the two test results is very low.

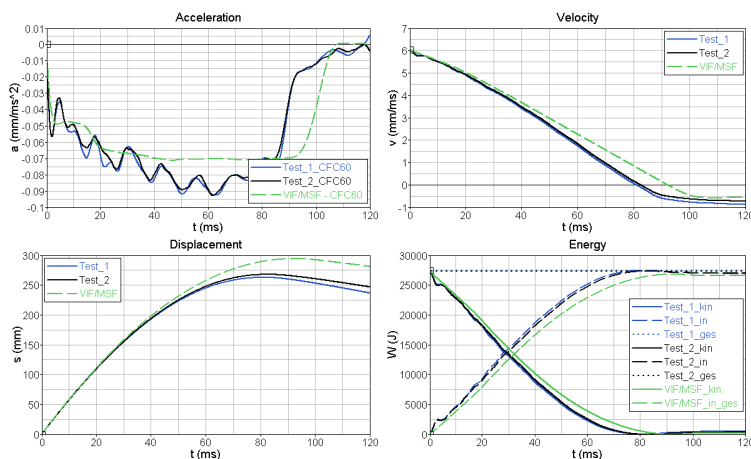


Figure 9: Comparison between test and simulation

The simulation model shows good correlation with the tests in the beginning. Starting from 20 ms the FEM model reaches a constant load level whereas the acceleration / force during the test is rising linearly. Due to less absorbed energy intrusion depth in simulation is higher. This effect can be seen even better with the acceleration plotted over displacement (figure 10)

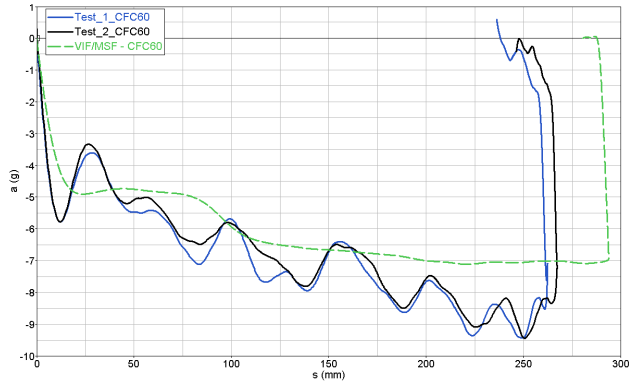


Figure 10: Comparison between test and simulation



Figure 11: Deformed barriers test 1, 2 and simulation;

A major difference between calculation and test is the performance of the upper unstruck area (figure 11). In reality the cells are rolled and compressed in T-direction behind the cladding. The FEM model shows a downward bending of the upper cells. A further point not yet implemented in the model is the additional force induced by the compressed air in the cells.

#### 4.2 Partial Overlap

For this test setup only two variants at the same Energy level were performed (table 2):

Table 2: Partial Overlap Test Conditions

Test No.	Mass [kg]	Velocity [kph]	Energy [kJ]
Test 5, 6:	1505.5	21.6	27.1
Test 7, 8:	2518.5	17.0	28.1

Again reproducibility of testing results is impressive. Though the displacement in simulation seems to fit fairly with the test data there is some discrepancy in the result as can be seen in the acceleration signal (figure 12).

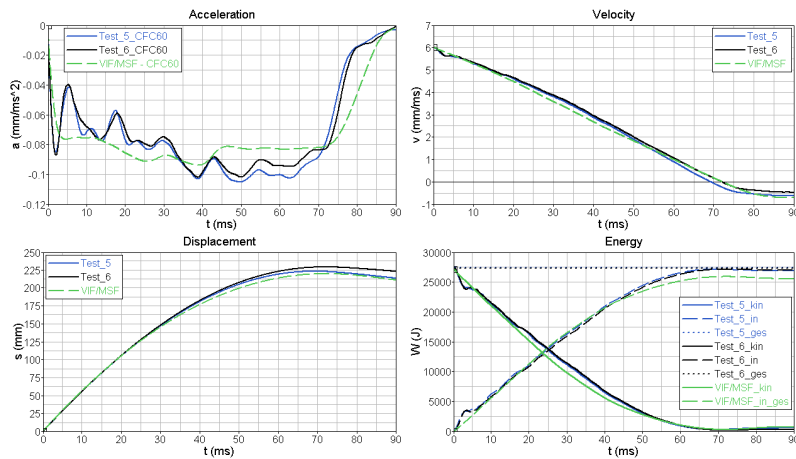


Figure 12: Comparison between test 5, 6 and simulation

As can be seen in figure 13 the force level is too high over a long intrusion distance. This is due to the fact that the gluing failure between cladding and main honeycomb occurs too late. Thus the bumper spreads the force widely and the main honeycomb absorbs too much energy. The so increased bending stiffness of the bumper leads in the following to the complete separation of the hit bumper parts from the unloaded ones. Therefore there is less force transfer to the not directly hit area of the barrier (figure 14), resulting in a lower force level compared with the test (figure 13, after 170mm deformation).

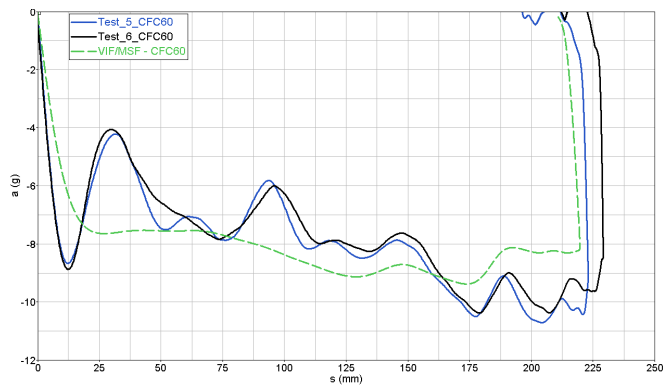


Figure 13: Comparison between test 5, 6 and simulation

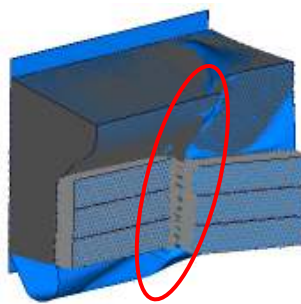


Figure 14: Deformed barriers test 5 and simulation;

Within this project it was not yet possible to find the correct definition of the glue. Failure either was too weak or too stiff especially respecting all the other test setups and also variances between different barriers. One reason for that is that currently there are only few glued contact points due to the macro cells with only six nodes per cell. In reality the glue supports the whole edge of the hexagon and not only the nodes defining the hexagon.

### 4.3 Local I-Beams

For this setup three different energies were tested (see table 3). Test 13 again aimed on a maximum deformation of the barrier whereas Test 9 and Test 10 only show little deformation and a wide energy transfer via the bumper into the whole main block of the barrier. The following pictures refer to test 13. As can be seen in figure 15 to 17 the DBM is not only able to allow high local intrusions in a stable manner but even predicts the force level quite well.

Table 3: Local I-Beam Test Conditions

Test No.	Mass [kg]	Velocity [kph]	Energy [kJ]
Test 9:	1498.5	9.4	5.1
Test 10:	1498.5	11.2	7.3
Test 13:	2512.5	17.0	28.1

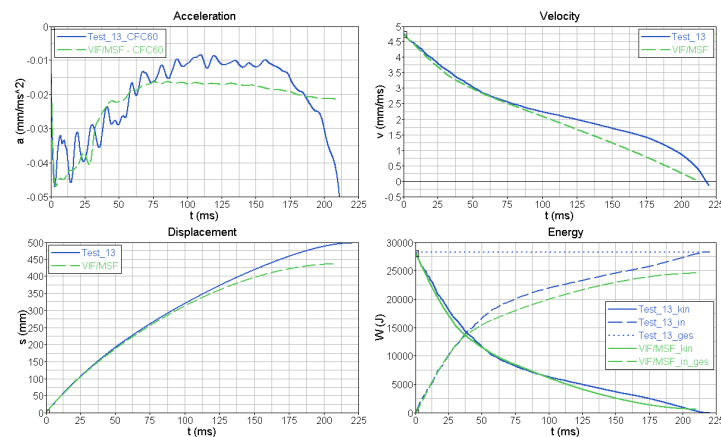


Figure 15: Comparison between test 13 and simulation

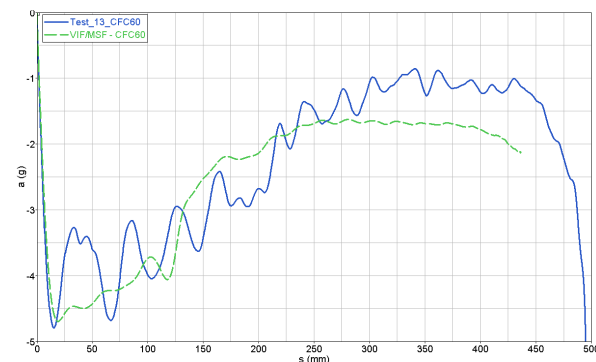


Figure 16: Comparison between test 13 and simulation

Failure of the cladding panels of main honeycomb and bumper are also represented in the correct way. This effect of very high but narrow deformations occurs even in real vehicle crash tests. Vehicles with a narrow / low front or with partial stiff components will split the barrier. Most of the energy will be absorbed by the vehicle when it hits the block behind the barrier.

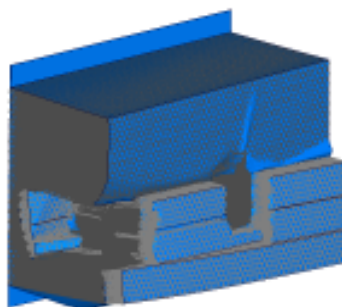


Figure 17: Deformed barriers test 13 and simulation;

## 5 Benchmark of Different Barrier Models

### 5.1 Barrier Tests

#### 5.1.1 Full overlap

To be able to judge the advantages and disadvantages of the new barrier concept it was compared to two different built FEM barrier models (BM1, BM2). As can be seen in figure 18 even these other barriers cannot describe the linear force increase in the full overlap test. The barriers are too weak and therefore deformation of the barriers is too high.

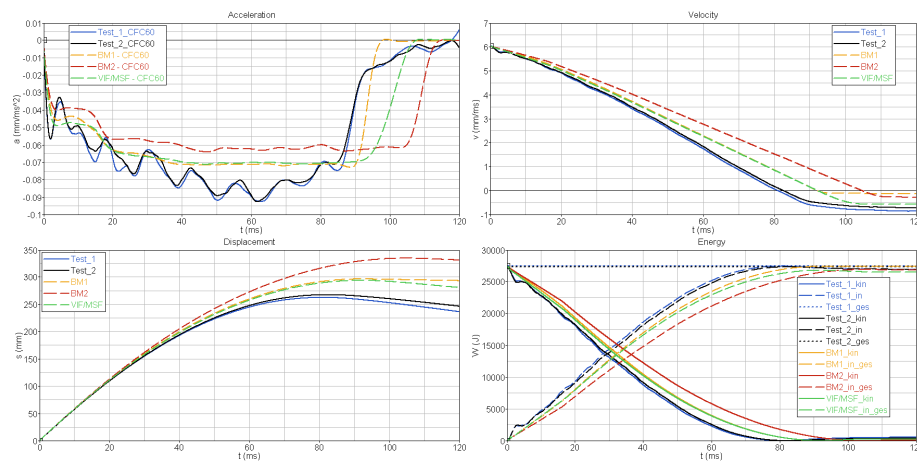


Figure 18: Comparison between test 5, 6 and simulation

It has to be mentioned that benchmark model 2 (BM2) was able to better represent the upper area that was not hit by the trolley. Though deformation looks better this barrier has also a constant force level and does not show the linear increase as in the tests. Furthermore it shows the lowest force level.

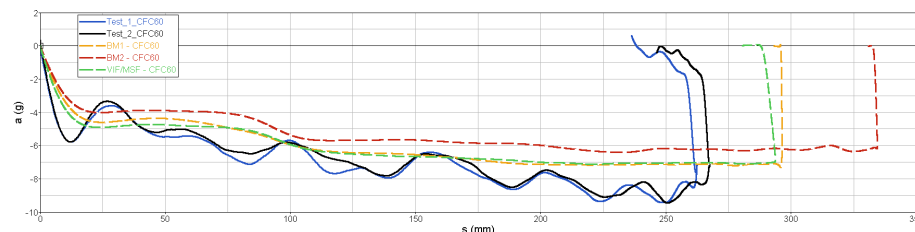


Figure 19: Comparison between test 5, 6 and simulation

#### 5.1.2 Local I-Beams

In this rather severe test the DBM shows its biggest advantage in comparison with the benchmark models BM1 and BM2. These models are not able to describe failure of aluminium honeycomb structures. Thus the characteristic deformation behaviour of the tested barrier is not shown. In contrast to the test the energy is distributed over the whole barrier and the observed displacement of the trolley is quite too low (figure 20 and figure 21).

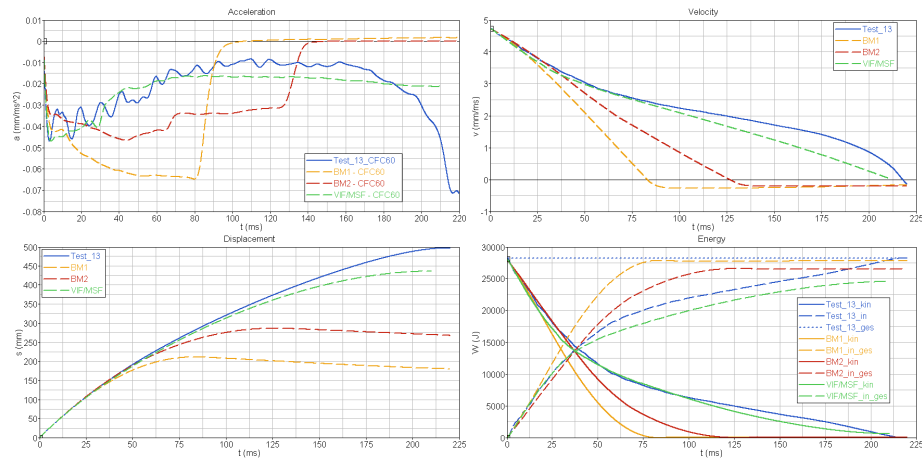


Figure 20: Comparison between test 13 and simulation

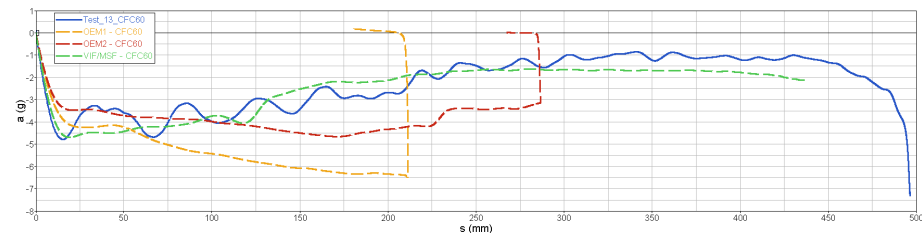


Figure 21: Comparison between test 13 and simulation

## 5.2 Full vehicle frontal crash

Looking on all the performed laboratory tests each of the three barriers had its advantages and disadvantages. Unlike the DBM barrier the benchmark models failed to show the correct physical deformation in some of the laboratory tests. But also did quite well in other tests. To leave those laboratory tests behind and to go one step closer to reality the same barriers were tested on an appropriate MAGNA b-segment concept vehicle for European markets. Though all the barriers showed different performances in the laboratory tests they all should represent one and the same real barrier type. In a supposed less severe test, like a full vehicle crash test, performances of the different barrier models should be comparable.

The following pictures (figure 22 to 24) on the left show a vertical section through a vehicles front rail. The right side represents a horizontal section through left and right front rail. The three models are overlaid to show the differences and can be distinguished by colours.

Table 4: Colour scheme for pictures below

DBM Magna Vif	green
BM1	orange
BM2	red



Figure 22: Vertical and horizontal section, time = 0 ms

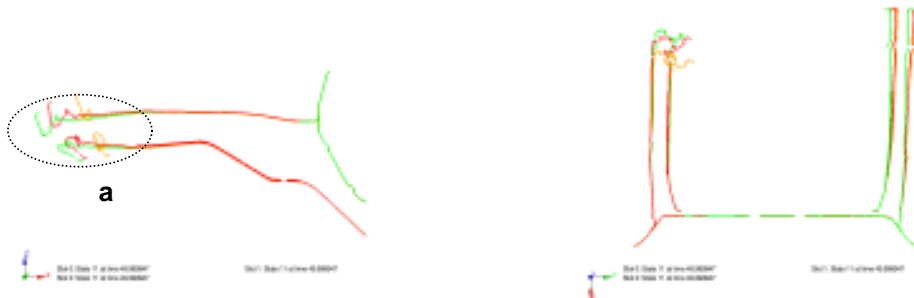


Figure 23: Vertical and horizontal section, time = 50 ms

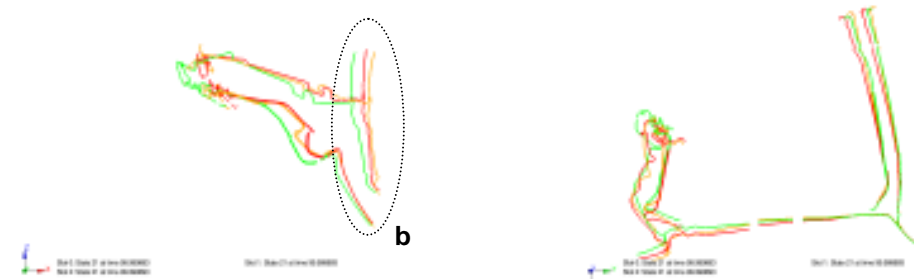


Figure 24: Vertical and horizontal section, time = 100 ms

Already in an early state of the crash simulation differences like a different triggering of the crash box and the pedestrian safety lower support occur (figure 23, a). Due to the different crash box behaviour the bending modes of the longitudinal are different as can be seen in figure 24. Differences pile up and finally firewall intrusions (figure 24b) are quite different. The behaviour of the firewall is of relevance for brake pedal and instrument panel movement and thus for the measured biomechanical values.

## 6 Conclusion

The new modelling method for honeycomb structures using discrete beams proved to be very efficient and accurate describing the specific structural behaviour. Especially stability under high relative deformations is outstanding. Local failure of the honeycomb structure can be predicted. Gluing and support of the cladding by the macro cells have to be further investigated although the current prototype has already now advantages over classical barrier models. A series of full vehicle crash calculations featuring different vehicle types ranging from sports cars to SUVs and a detailed comparison with the real crash test (laser scan of vehicle and barrier) would emphasise the capabilities of this new barrier formulation and underline the results presented in this paper.

Laboratory tests as shown in this paper can help to judge the quality of different barrier models in any FEM code. Since also robustness of the developed vehicles regarding their performance in slightly modified setups is required it seems to be helpful to vary the barrier model.

The barrier is only one element of a chain leading to the biomechanical properties during a crash test. Only by optimisation of all the elements like material properties, representation of joinings, failure description and optimised dummies and interface descriptions a reliable prognosis quality can be achieved. The DBM barrier model will be part of the VALIDATED VIRTUAL DEVELOPMENT process at MAGNA STEYR.

## 7 Acknowledgement

The authors would like to thank the "Kplus Kompetenzzentren-Programm" of the Austrian Federal Ministry for Transport, Innovation, and Technology (BMVIT), Österreichische Forschungsförderungsgesellschaft mbH (FFG), Das Land Steiermark, and the Steirische Wirtschaftsförderung (SFG) for their financial support. Additionally we would like to thank the supporting companies and project partners Virtual Vehicle - Competence Center and the Graz University of Technology.

## 8 Literature

- [1] Statistisches Bundesamt Deutschland, url: [http://www.destatis.de/jetspeed/portal/cms/Sites/destatis/Internet/DE/Presse/pm/2009/02/PD09\\_063\\_46241,templateld=renderPrint.psmI](http://www.destatis.de/jetspeed/portal/cms/Sites/destatis/Internet/DE/Presse/pm/2009/02/PD09_063_46241,templateld=renderPrint.psmI), (April 2009)
- [2] Insurance Institute for Highway Safety, "Side Impact Crashworthiness Evaluation - Crash Test Protocol (Version V)", url: [http://www.iihs.org/ratings/protocols/pdf/test\\_protocol\\_side.pdf](http://www.iihs.org/ratings/protocols/pdf/test_protocol_side.pdf), (April 2009)
- [3] Wagner, U., Annandale, R., Wüstner, H.; Winkelmueller G.: "Erhöhte Anforderungen für Berechnungsmodelle im Entwicklungsprozess am Beispiel der deformierbaren Barriere", VDI Berichte Nr.1283, 1996, S.237-249
- [4] Gibson, L., Ashby, M.: "Cellular Solids", 2<sup>nd</sup> Edition, Cambridge, Cambridge University Press, 1997
- [5] Wierzbicki, T.: "Crushing Analysis of Metal Honeycombs", Int. J. Impact Engng. Vol.1 No.2, 1983, S.157-174
- [6] Klintworth, J., Stronge, W.: "Elasto-Plastic Yield Limits and Transversely Crushed Honeycombs", Int. J. Mech. Sci. Vol.30 No.3/4, 1988, S.273-292
- [7] Zhou, Q., Mayer, R.: "Characterization of Aluminium Honeycomb Material Failure in Large Deformation Compression, Shear, and Tearing", Journal of Engineering Materials and Technology Vol.124, 2002, S.412-420
- [8] Walker, B.; Bruce I., Tattersall P., Asadi M.: "A New Generation of Crash Barrier Models for LS-DYNA", 5. LS-DYNA Anwenderforum, Ulm, 2006, Session B-II, p. 15-35
- [9] Shkolnikov, M.: "Honeycomb Modeling for Side Impact Moving Deformable Barrier (MDB)", 7<sup>th</sup> International LS-DYNA Users Conference; Detroit, 2002, Session Crash/Safety (2), p. 7.1-7.14
- [10] Tryland, T.: "Alternative Models of the Offset and Side Impact Deformable Barriers", 9<sup>th</sup> International LS-DYNA Users Conference, Detroit, 2006, Session Crash/Safety (1), p. 1.9-1.16
- [11] Kojima, S., Yasuki, T., Oono, K.: "Application of Shell Honeycomb Model to IIHS MDB Model", 6<sup>th</sup> European LS-DYNA Users Conference, Gothenburg, 2007, Session 1.3.1, p. 1.71-1.80
- [12] Jost, T., Heubrandtner, T., Ruff, C., Fellner, B.: „A New Method to Model Aluminium Honeycomb Based Crash Barriers in Lateral and Frontal Crash Load Cases“, 7th German LS-Dyna Forum '08, Bamberg, Crash III - Failure / Barriers, B-III p.13-23
- [13] Winklhofer, J., Trattig, G., Schluder, H., Fellner, B.: „Effiziente Ermittlung von Dehnraten- und Versagensparametern für die Fahrzeug-Crashsimulation mit LS-DYNA“, 7th German LS-Dyna Forum 2008, Bamberg, Session Crash II - Conncetions / Failure, B-II p- 35-46